ELSEVIER

Carbohydrate Polymers 40 (1999) 115–124

Carbohydrate Polymers

# Structural aspects in ultrathin cellulose microfibrils followed by $^{13}C$ CP-MAS NMR

L. Heux*, E. Dinand, M.R. Vignon

*Centre de Recherches sur les Macromolécules Végétales CERMAV-CNRS, Joseph Fourier University of Grenoble, B.P. 53, 38041 Grenoble Cedex 9, France*

Received 17 August 1998; received in revised form 22 February 1999; accepted 1 March 1999

**Abstract**

$^{13}C$ CP-MAS NMR was used to study the ultrastructural aspects of ultrathin microfibrils extracted from sugar beet pulp. Depending on the stocking condition, the cellulose microfibrils contained different amounts of the polymorphs Iα and Iβ. Structural changes were followed after a purification treatment. It was found that the crystallinity, as measured by solid-state NMR, increases as the purification proceeds. This is primarily due to the removal of non-cellulosic polysaccharides during the different treatments. This was confirmed by neutral sugar analysis. A crystallite size of 4 nm is derived from the NMR results which is in good agreement with the TEM observations. To avoid any underestimate of the microfibrils size, most of the hemicelluloses tightly bound to the cellulose microfibrils has to be removed. 

*Keywords:* Cellulose microfibrils; Sugar beet pulp; *Valonia*

## 1. Introduction

During the past decade, high resolution solid state NMR has proven to be a powerful tool in the investigation of structural features of cellulosic materials. The primary field of interest is the crystalline ultrastructure of cellulose, which differs in many aspects from synthetic polymers. The biosynthesis of the cellulose leads to monocrystals, in the shape of slender rods called microfibrils, with very high aspect ratios, instead of platelets or lamellae, the shapes commonly encountered with synthetic polymers. Moreover, the high sensitivity of the chemical shift of cellulose to the surroundings has allowed ordered and disordered cellulose to be differentiated (Earl & VanderHart, 1981; Maciel, Kolodododziejski, Bertran & Dale, 1982) by the very well-separated lines for the so-called C6 and C4 of the glucosyl moieties. Relative areas under these peaks have then been used to evaluate the degree of crystallinity, showing results in good agreement with X-ray diffraction data (Horii, Yamamoto, Kitamaru, Tanahashi & Higuchi, 1987; Teeäär, Serimaa & Paakkari, 1987). One can also take advantage of the differences in $^{13}C$ spin relaxation times $T_{1C}$, which are longer in the crystalline components than in the non-crystalline part of the material (Pfeffer, 1984). Newman has also proposed a method based on the differences in proton spin relaxation times in the rotating frame $T_{1\rho}$ ($^{1}H$) by a decomposition in sub-spectra (Newman & Hemmingson, 1990, 1994). However, the exact assignment of the signals, especially in the case of the C4 line is still a matter of controversy (Larsson, Wickholm & Iversen, 1997). Despite the apparent multiplicity of the signals arising from the disordered regions, it is nevertheless possible to evaluate an "apparent crystallinity index" by integrating in the amorphous part of cellulose all contributions arising from the disordered regions, i.e. surface chains, crystal defects and amorphous material, including hemicelluloses.

High resolution solid state NMR also enables various crystalline allomorphs of cellulose (I–IV) to be distinguished. The existence of two different crystalline forms in native cellulose, Iα and Iβ, was first demonstrated by CP-MAS (Attala & VanderHart, 1984; VanderHart & Atalla, 1984) and then further confirmed by electron diffraction and FTIR (Sugiyama, Persson & Chanzy, 1991). A recent review (O'Sullivan, 1997) described in detail the precise features of the various studies dealing with cellulose polymorphism.

So far, most of the NMR work related to the cellulose polymorphism has dealt with highly crystalline samples like *Valonia*, tunicin or cotton secondary walls because of the better resolution obtained with such ordered samples. As they represent a non-negligible part of the biomass, cellulose contained in annual plants is of great interest despite its

* Corresponding author.

0144-8617/99/$ - see front matter 
PII: S0144-8617(99)00051-X

generally poorer crystallinity. A recent study on fern cellulose (Newman, 1997) has already proved that polymorphism can be studied in such samples.

This work will focus on the cellulosic material extracted from sugar beet pulp (SBP), which corresponds to the material left after the removal of saccharose from sugar beet roots. Sugar industries produce large amounts of pulps that are at this moment mainly used in cattle-feed. In order to develop new routes of valorization, a purification process of these pulps to obtain a cellulose-rich product in the form of ultrathin microfibrils has been described recently (Dinand, Chanzy, Vignon, Vincent & Maureaux, 1995; Dinand, Chanzy & Vignon, 1996). In this work, the polymorphism of these microfibrils depending on their origin and storage conditions is studied. Moreover, the high ratio of surface area to volume allows efficient study of slight changes occurring at the surface of the crystallites. Such studies are almost impossible on highly crystalline samples. Although it is difficult to get NMR data which can be easily interpreted, we were able to monitor the structural changes of cellulosic samples from sugar beet pulp during its purification process. Indeed, both "apparent crystallinity index" and allomorphic ratios are evaluated at different purification stages of SBP processing.

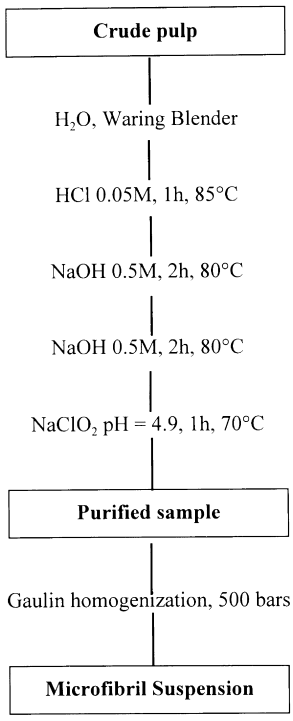


Fig. 1. Purification process of the sugar beet pulp.

## 2. Experimental

### 2.1. Materials

Sugar beet pulp was supplied by Saint-Louis Sucre (Nassandres, France). After harvesting and sugar extraction of the sugar beet roots, the beet pulps are either desiccated at high temperatures and stored, or ensiled under large plastic sheets for further use. The different steps of the purification process are presented in Fig. 1. The crude pulp was dispersed in distilled water (10 g of equivalent dried matter in 500 ml) for 15 min in a Waring Blender at full speed. This suspension was shaken for 2 h at room temperature and filtered in order to remove the residual saccharose and water soluble pectins. An acidic extraction was then performed with a 0.05 M HCl solution for 1 h at 85°C, and the suspension was filtered and washed extensively on a 25 μm Blutex cheesecloth (Tripette et Renaud, France). The residual product was resuspended into 0.5 M NaOH solution and shaken for 2 h at 80°C, filtered and washed with distilled water. The NaOH extraction was performed twice. The alkali-insoluble residue was bleached twice with sodium chlorite at 70°C for 1 h according to Dinand et al. (1996).

### 2.2. Sugar analysis

The uronic acid content was determined by the *m*-hydroxydiphenyl method, according to Blumenkrantz & Asboe (1973). Neutral sugars were released by Saeman hydrolysis and quantified by GLC as their corresponding alditol acetates (Selvendran, March & Ring, 1979), using a Packard and Becker 417 instrument coupled to a Hewlett-Packard 3380A integrator. A glass column (3 mm × 2 m) packed with 3% SP 2340 on Chromosorb W-AW DMCS (100–120 mesh) was used.

### 2.3. Preparation of microfibril suspensions

The purified SBP, at 1–2% concentration in water was treated for 15 min in a Waring Blender (18 000 rpm), where a final temperature of 60°C was reached. The sample was immediately homogenized by 15 passes through a Manton Gaulin laboratory homogenizer (15MR-8TBA) operated at 500 bars.

### 2.4. Solid state NMR

The NMR experiments were performed on a Bruker MSL spectrometer operated at a $^{13}C$ frequency of 25 MHz using the combined technique of proton dipolar decoupling (DD), magic angle spinning (MAS) and cross-polarization (CP). $^{13}C$ and $^{1}H$ field strengths of 64 kHz corresponding to 90° pulses of 4 μs were used for the matched spin-lock cross-polarization transfer. The spinning speed was set at 3000 Hz for all the samples. The contact time was 1 ms, the acquisition time 70 ms, the sweep width 29 400 Hz and the recycle delay 4 s. A typical number of 10 000 scans were acquired for each spectrum. When specified, enhanced spectra were obtained by a gaussian broadening GB = 0.5 and line broadening LB = − 30 Hz.

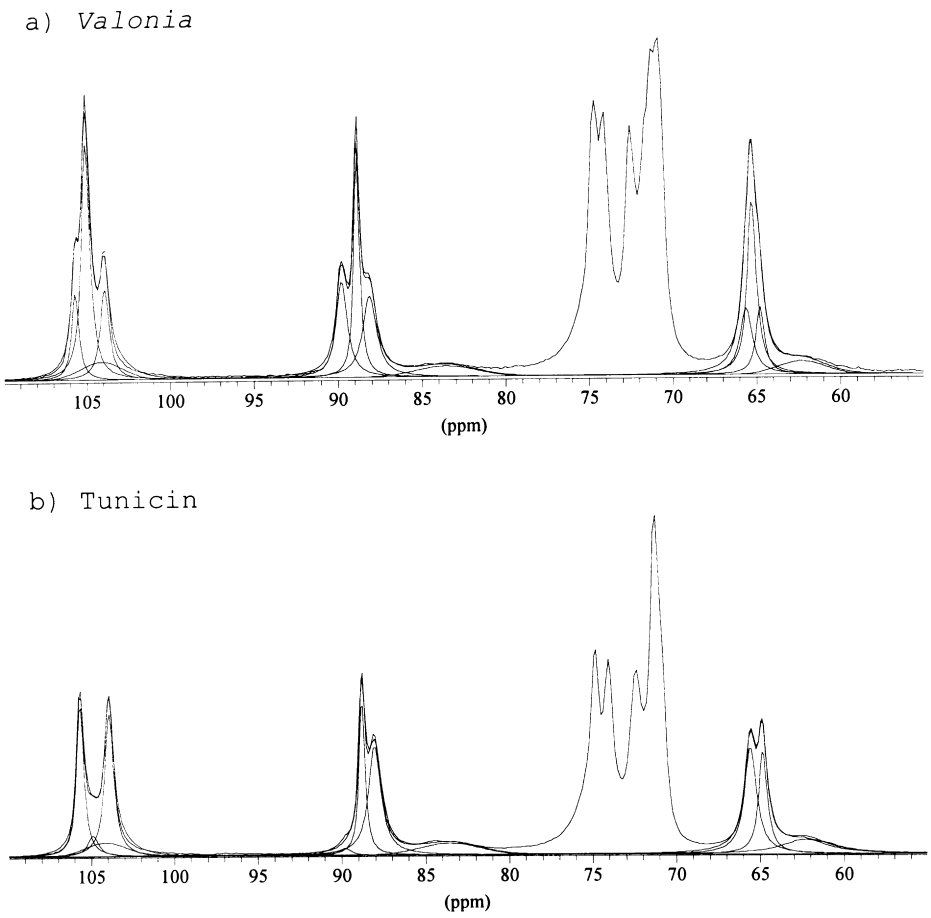


Fig. 2. Line-shape analysis: (a) *Valonia*; (b) Tunicin.

### 2.5. NMR methodology

Due to their very small lateral size, ranging from 1.5 to 4 nm, the SBP microfibrils are somewhat difficult to study. The first reason is the presence of a small amount of hemicelluloses and residual pectic polysaccharides as incrustants at the surface of the microfibrils (Dinand et al., 1996). The very high ratio of surface to volume makes this contribution non-negligible and easily observable. The lines arising from these incrustants appear as an additional contribution to those from the disordered regions. The other difficulty is the broadness of the crystalline lines in the spectra of such samples, due to the small lateral size of the microfibrils. One can use the well-known chemometric methods used by Lenholm, Larsson and Iversen (1994). However, this method is not easily performed. One can take advantage of the difference in relaxation times ($T_{1C}$) between amorphous and crystalline part to differentiate the corresponding signals. This method, in the case of $T_{1C}$, is time consuming, and not entirely accurate for quantification purposes. It is therefore advantageous to use a simple but precise deconvolution procedure based on the analysis of model compounds such as *Valonia* and tunicin.

### 2.6. Quantitative NMR measurements

Special care was taken for the quantitative analysis of the NMR measurements. The recycle delay was set to a value long enough to avoid the effect of $T_1$ relaxation in the relative areas of the peaks. This was checked on every sample. By following the cross-polarization kinetics, it was found that the optimum contact time was 1 ms. Lower and higher values of the contact time are problematic, as each constituent (crystal interior, surface, hemicelluloses) has different $T_{CH}$ and $T_{1\rho}$ ($^1$H). As long as we are not interested in the C6 carbons, $T_{1\rho}$ ($^{13}$C) should not be a problem for the quantitative measurements of the intensities (Hill, Le & Whittaker, 1994). Moistening of the cellulosic samples with excess water is commonly used to enhance the mobility of the disordered regions, and then, to improve artificially the resolution. In this study, dried samples were used for two reasons. First, it is not completely clear whether the CP efficiency will be the same for each type of carbon, and that the water content will not decrease during the experiment. Second, as lines arising from some type of disordered regions become narrower, it is more difficult to separate them from the crystalline signals, especially in the C1

Table 1
Crystallinity indices and allomorphic ratios obtained on the spectra of model celluloses

| Samples | *Valonia* | *Valonia*[a] | Tunicine | Tunicine[a] |
|---|---|---|---|---|
| Crystallinity indice[b] | 0.82 | 0.88 | 0.78 | 0.85 |
| Allomorphic ratio Iβ/Iα[c] | 0.42 | 0.38 | 0.93 | 0.89 |

[a] Enhanced spectra with a Gaussian broadening GB = 50.
[b] Estimated from the ratio between the area of the line at 83.5 ppm and the area of the crystalline lines at 89.8, 88.8 and 88.1 ppm.
[c] Estimated from the ratio between the area of the lines at 105.7 and 103.9 ppm (Iβ) and 105.0 ppm (Iα).

region, which is of particular interest for the allomorphism evaluation.

### 2.7. Calibration by model compounds

Owing to their low crystallinity, the SBP microfibrils do not present narrow peaks characteristic of highly crystalline samples. For this reason, highly crystalline materials were used as model compounds to calibrate our methodology, i.e. *Valonia* cellulose with a high Iα content and tunicin cellulose which contains almost exclusively the Iβ phase. The spectra are shown in Fig. 2 together with the signal deconvolutions. The chemical shifts and the multiplicity of the peaks of each allomorph (Iα, Iβ) and those for the disordered contribution are very well known. It is noteworthy that each carbon signal can provide interesting information: anomeric C1 signals allow us to determine the Iβ/Iα ratio (signals at 105.7, 104.0 and 105.1 ppm respectively); C4 signals resonating between 80–85 ppm are used for the calculation of the amount of disordered region (Newman, Davies & Harris, 1996). Results found for the allomorphic ratios Iβ/Iα are shown in Table 1. They are determined from the integrations of the C1 lines, which have been unambiguously identified and fit with lorentzian lineshapes. Gaussian lineshapes are used for the disordered contributions. The results found for both *Valonia* and tunicin are in very good agreement with those found in the literature (Larsson, Westermark & Iversen, 1995; Yamamoto & Horii, 1993). The height of the disordered contribution to the C1 peak was set such as its area equalized the area of the disordered contribution to the C4 peak. Indeed, as cellulose is a β 1 → 4 glucan, it is reasonable to postulate that there is as much C1 as C4 in these disordered regions.

Additionally, it is very well known that quantitativity is lost during the resolution enhancement apodization (Ferrige & Lindon, 1978). It is then impossible to evaluate crystalline indices from the enhanced spectra. Considering the

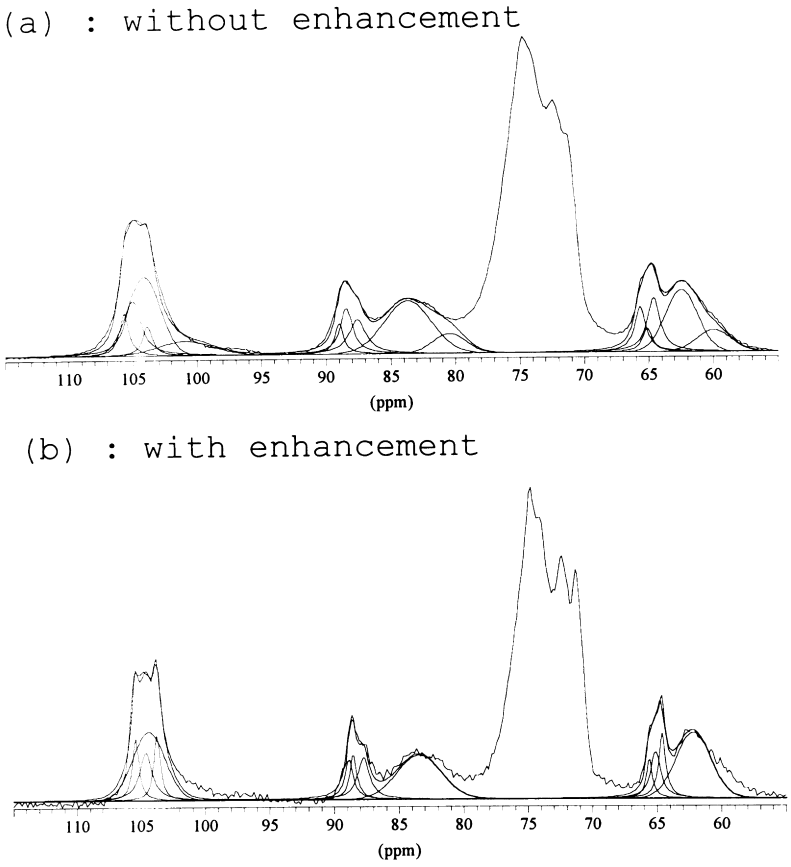


Fig. 3. Line-shape analysis of purified SBP microfibrils: (a) without enhancement; (b) with enhancement.

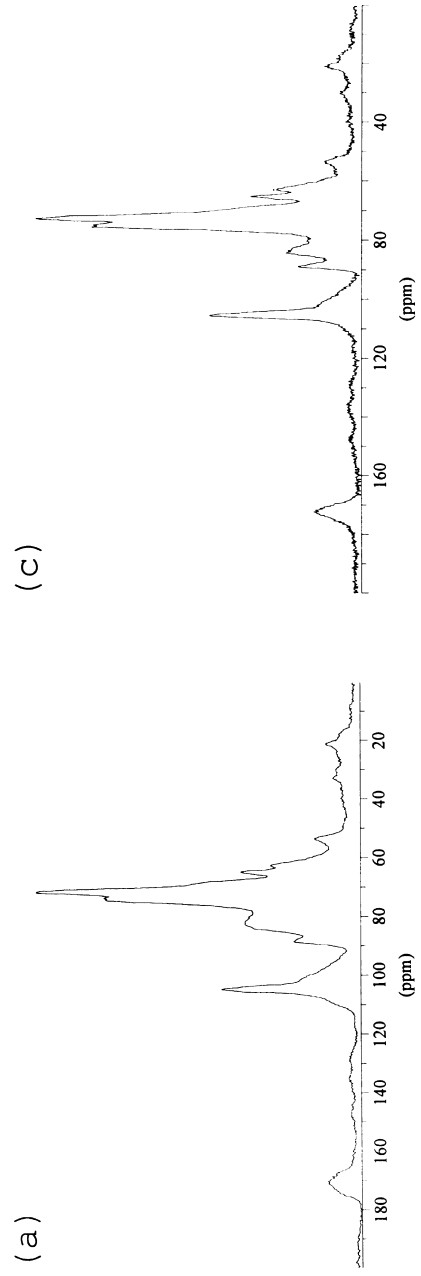


Fig. 4. CP-MAS $^{13}$C-NMR spectra of SBP: (a) crude pulp; (b) after water extraction; (c) after acid treatment HCl 0.05 M; (d) after alkali treatment NaOH 0.5 M.

Table 2
Neutral sugar analysis of SBP samples before and after acidic treatment (figures given here are the mass percentage of each neutral sugar on the total amount of neutral sugars detected. t is trace, not determined)

| Sugar | Glucose | Galactose | Mannose | Xylose | Arabinose | Fucose | Rhamnose |
|---|---|---|---|---|---|---|---|
| Before $H^+$ | 74 | 2 | 5 | 12 | 6 | 0.7 | 0.3 |
| After $H^+$ | 91 | t | 4 | 4 | 1 | t | t |

crystalline contribution, the linewidths are divided by a 1.5 factor. However, as shown in Table 1, the allomorphic ratios are only slightly changed.

### 2.8. Signal treatment on SBP spectra

A typical spectrum of SBP is shown in Fig. 3(a). As discussed previously, the poor crystallinity induced considerable line broadening. The enhanced spectrum shown in Fig. 3(b) is much better defined. Nevertheless, the relative larger amount of disordered regions makes the deconvolution of the C1 peak difficult. By analogy to the successful calibration with the model compound, we then proceed in the following manner. Positions and line widths of the crystalline peaks are measured from the deconvolution of the enhanced spectra. These values are used for the deconvolution of the untreated spectra, providing a 1.5 multiplication of the line widths. The other constraint is then the allomorphic ratio. The same set of width and position of the peaks has been used for all the samples, the possible error would at be least systematic. Finally, a second disordered line is necessary to account for the high field part of the C1 and C4 lines. This additional contribution arises from the hemicelluloses tightly bound to the surface of the microfibrils and is added to the disordered contribution.

## 3. Results

### 3.1. First purification of sugar beet pulp

The raw SBP consists mainly of pectins (25–30%), hemicelluloses (25–30%) and cellulose (20–25%), which have signal resonances with close chemical shifts. For this reason the NMR spectra showed broad and overlapping signals. The precise analysis in terms of deconvolution was therefore achieved after the removal of pectins, most of hemicelluloses and other minor components. The spectra shown in Fig. 4(a)–(d) were obtained: (i) on the raw material, (ii) after a water extraction, which removed hydrosoluble pectins, (iii) after an acid treatment with HCl 0.05 M, which hydrolyzed some branched pectins, and (iv) after an alkali treatment with NaOH 0.5 M, which solubilized the remaining pectins and most of the hemicelluloses. At this stage, the disencrusted SBP cells appeared as individualized cell-ghosts corresponding to the flattened cell envelopes. The neutral sugar analysis shown in Table 2 gave a glucose content of 74%, indicating that cellulose was the major component. However, there is a substantial amount of hemicellulose left containing xylose, arabinose and mannose. The lines arising from these sugars contribute to the disordered region of cellulose and to the aforementioned additional shoulders at higher fields.

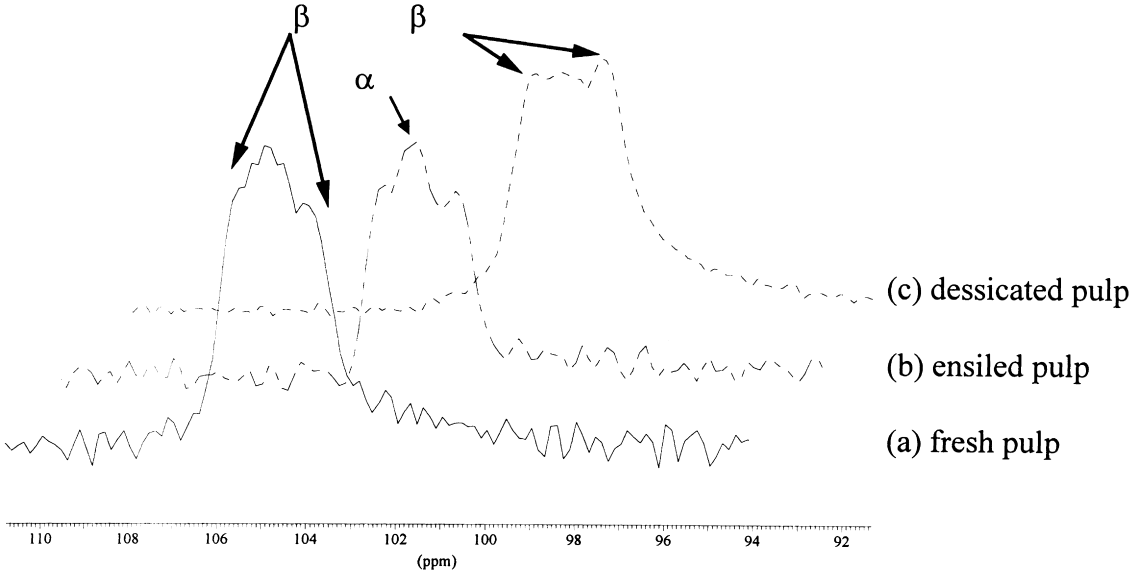


Fig. 5. C1 region of enhanced CP-MAS $^{13}$C-NMR spectra of SBP: (a) fresh pulp; (b) ensiled pulps; (c) desiccated pulp.

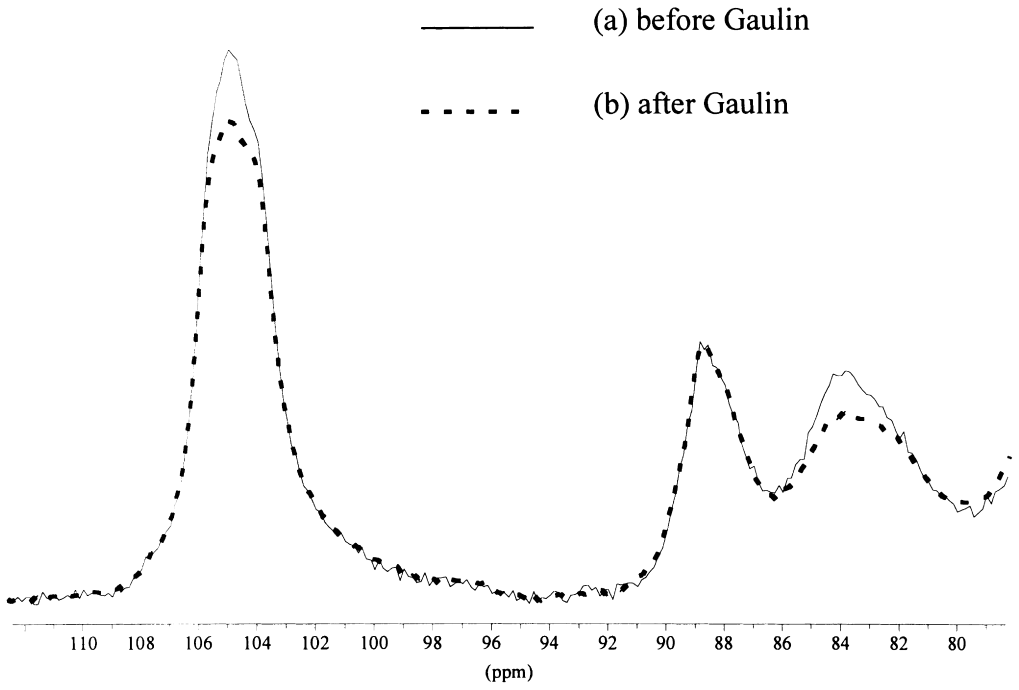


Fig. 6. C1 and C4 region of CP-MAS $^{13}$C-NMR spectra of purified SBP: (a) —before Manton Gaulin homogenization; (b) – – – – – after Manton Gaulin homogenization.

### *3.2. Effect of the origin and of the storage of sugar beet pulps*

SBP were studied either as fresh pulp or ensiled pulp, and after a desiccation process. Desiccation is a dramatic treatment that is known to lead to the hornification of polysaccharides and cellulose (Laivins & Scallan, 1993). The total amount of disordered material does not differ very much among the three samples, indicating that the microfibrils size and environment did not change drastically during the desiccation or the storage. Nevertheless, it is worth noting that the allomorphic proportion changed from 40% of Iβ phase in the fresh pulp and silage to 55% in the desiccated materials. These ratios have been measured on over ten samples either desiccated or ensiled at different stages of purification and do not differ with further purification treatment. Fig. 5 illustrates the changes observed in the C1 peak for these three types of samples. Even if the deconvolution does not lead to very precise values, it is undeniable that there is a quantitative change in the allomorphic ratio during the desiccation step. Similar transformations have been already observed, for example with *Valonia* samples after a saturated steam treatment at high temperature (Horii et al., 1987). Our results can be similarly explained by the relaxation of deformed or distorted zones in the cellulose microfibrils upon wetting. Moreover, this observation is consistent with the fact that the Iα phase is less stable than the Iβ phase and that it can be converted into Iβ during a severe treatment of the microfibrils. The origin of the sample, and its storage and processing conditions are thus of great importance. These results also prove that our methodology is reliable. All the other experiments have been performed on the desiccated samples.

### *3.3. Effect of mechanical treatment*

The disencrusted cells (purified sample, Fig. 1) are disrupted by passing several times through a Manton Gaulin homogenizer. This treatment leads to both individual and small bundles of microfibrils. SBP samples were compared before and after this drastic mechanical treatment. CP-MAS spectra obtained prior and after the Manton Gaulin processing are shown in Fig. 6. The decrease of the intensity of the disordered contribution to the C4 peak at 83 ppm indicates that the crystallinity index increases during the mechanical process. Additionally, the overall intensity of the C1 peak decreases as its disordered contribution decreases. Integration of the spectral lines confirms this result with 32 and 38% of crystallinity before and after treatment. These results are in good agreement with those obtained by Wormald, Wickholm, Larsson and Iversen (1996), who observed a conversion between disordered and ordered cellulose upon mechanical treatment followed by cycles of wetting and drying on *Cladophora* and microcrystalline celluloses. This observation suggests that some constrained parts of the microfibrils, previously appearing as disordered material have been cut during the mechanical process. These parts can then reorganize into crystals, due to the increased mobility provided by water.

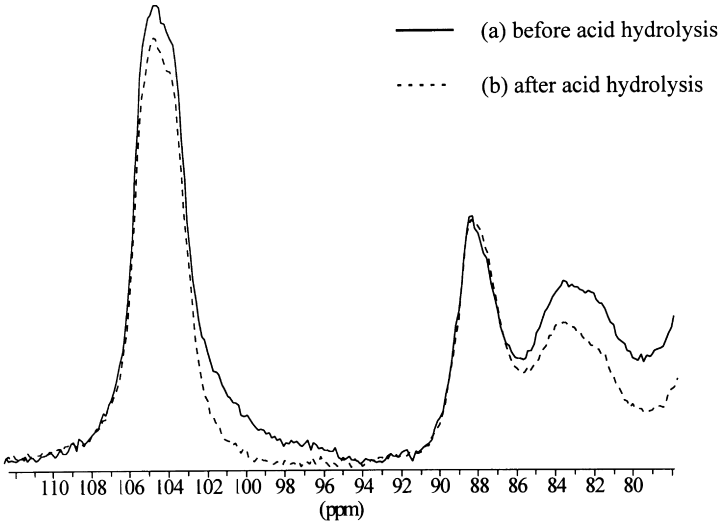


Fig. 7. C1 and C4 region of CP-MAS $^{13}$C-NMR spectra of SBP: (a) before acid hydrolysis; (b) after acid hydrolysis.

### 3.4. Effect of acid hydrolysis

For further purification, one can use either an alkaline or an acidic treatment. Fig. 7 displays the spectra obtained for SBP microfibrils before and after a 1.5 h treatment in a 1 M HCl solution at 80°C. This treatment leads to a noticeable decrease in the peak height from the disordered areas. Consequently, the crystallinity indices deduced from the deconvolution of the spectra are 0.38 and 0.47 respectively. Because such a mild hydrolytic treatment does not increase the microfibrilar size, one can assume that the lost material is non-cellulosic polysaccharides which have a strong interaction with cellulose at the microfibrils surface. The analysis of the neutral sugar, shown in Table 2 before and after acid hydrolysis, indicates that the total amount of neutral sugars other than glucose drops from 26 to 9%. These neutral sugars correspond to hemicelluloses released during the acidic treatment. As the chemical shifts of these hemicelluloses correspond to those of disordered cellulose, the main effect of these surface polysaccharides is to decrease the crystallinity index, and leading to an underestimation of the actual size of the microfibrils. Additionally, the sugar analysis shows that xyloglucans, glucomannans or glucuronoxylans are probably the hemicelluloses which are most tightly bound to cellulose.

### 3.5. Evaluation of the microfibrils size

All the previous results are important for two reasons. First, they prove that the microfibrils are covered by polysaccharides tightly bound to the surface of the microfibrils. Second, if these polysaccharides were removed, the disordered contribution would only originate from the surface chains. The crystallinity indices can then be related to the size of the microfibrils. Considering that the acidic treatment leads to a microfibril containing 92% cellulose and assuming that the crystalline core contains only cellulose, the real crystallinity index can be estimated roughly as 0.51. The number of chains in the interior of the crystal can then be calculated, assuming a square microfibril section of $(n + 2)$ chains per side and an infinite longitudinal size. The chain number in the crystalline core of the crystallite is $n^2$ and $r$ is the typical ratio of the crystalline core to the total amount of cellulose. This ratio is equivalent to the crystalline index evaluated from solid state NMR measurements. The following formula is easily obtained:

$$r = \left(\frac{n}{n+2}\right)^2$$

or

$$n = 2\frac{r + \sqrt{r}}{1 - r}.$$

With a crystallinity index of 0.51, we then calculate an average number of 25 chains belonging to the interior of the crystal microfibril, i.e. 5 chains square in the crystalline core of the microfibril. Assuming an average interchain distance of 0.58 nm, this represents an external lateral size of approximately 4 nm and an internal diameter of the crystalline core around 3 nm. This result is in good agreement with the observation of the purified SBP microfibrils by Transmission Electron Microscopy (TEM) (Dinand et al., 1996). Nevertheless, it is postulated in this model that the surface effect influences only the thickness of one chain. Moreover, the purification stage of the microfibrils is obviously crucial for the size evaluation. In this SBP sample, before hydrolysis and removal of the polysaccharides adsorbed on the surface of the microfibrils, we found an apparent crystallinity index of 0.38, leading to an apparent average external size of 3 nm. This result would have been an underestimate of the actual size of the microfibrils.

## 4. Discussion

Lineshape analysis of solid state NMR spectra has allowed us to monitor some structural features of the microfibrils during their purification process. Structural and morphological changes can be deduced from the solid state NMR observations. After the first chemical purification stages, the microfibrils are disencrusted and most of the hemicelluloses and pectins have been removed. The mechanical treatment leads to a partial individualization of the microfibrils, destroying defects such as kinks and twists along the microfibrils. These reorganizations enable an apparent increase in the NMR crystallinity index. After a mild acid hydrolysis, some of the polysaccharides tightly bound onto the surface can be removed, leading to a further apparent increase in the NMR crystallinity index. A crystallite size of 4 nm can then be predicted, leading to lateral sizes comparable with TEM observation. The poor crystallinity of the primary cell-wall cellulose is very well-known (Frey-Wyssling, 1954), and previous authors have found crystallinity indices by solid state NMR as low as 0.40 for the cellulose in the primary cell-wall of apple fruit (Newman, Ha & Melton, 1994) or *Arabidopsis thaliana* leaves (Newman et al., 1996). It appears from our study that microfibrils of primary cell-walls of monocotyledon, such as sugar beet root, could have crystallinities slightly higher than 40%, which means that microfibrils have larger lateral sizes than believed or that purification process has proceeded further. Several authors have discussed the inherent differences in the crystallinity indices evaluated by X-ray diffraction and solid state NMR. With X-ray diffraction, a measurement of low crystallinity indicates small crystallite dimensions, whereas with NMR, this result indicates a large amount of non-crystalline material. Solid state NMR allows one to study ultrathin microfibrils, which are difficult to study by X-ray diffraction, and to determine the presence and evolution of amorphous polysaccharides bound to the surface. These polysaccharides, most probably hemicelluloses, are undectectable with X-ray diffraction as they are not crystalline.

Our experiments illustrate these aspects by the constant increase of the crystallinity indices measured by NMR during the purification process, whereas the size of the microfibrils remain unchanged. Moreover, our results outline the difficulty of using the crystallinity index determined by NMR to measure an apparent crystal lateral size, without checking the efficiency of the purification process. The very small lateral size of the SBP microfibrils lead to very broad X-ray patterns, commonly called cellulose $IV_I$ (Chanzy, Imada & Vuong, 1978; Chanzy, Imada, Mollard, Vuong & Barnoud, 1979). Although the NMR analysis of ultrathin microfibrils is much more difficult than for more crystalline samples, our experiments show that the crystalline packing is probably the same in cellulose I and $IV_I$. Indeed, the chemical shifts in the Iα and Iβ phases of the SBP microfibrils are identical to those of the other well known samples, such as the highly crystalline *Valonia*.

## 5. Conclusions

In this article, we have shown that solid state NMR, when carefully used, can provide interesting features concerning the structural modification of ultrathin microfibrils originating from parenchyma cell walls. It was shown that the measurement of crystallinity indices should be considered with caution. Indeed, they yield useful information on the state of the microfibrils, for example during a purification process. However the full removal of polysaccharides interacting with the cellulose chains at the surface of the microfibrils has to be verified before getting a dimensional quantity from this measurement. Even in this case, extreme care should be taken before extracting characteristic dimensions from the NMR results. NMR crystallinity indices have to be confronted with the results from TEM observation and sugar analysis. In this context, we were able to understand and follow the structural changes occurring in ultrathin objects such as sugar beet root microfibrils during their purification process, and to control precisely each step of the treatment.

## Acknowledgements

We thank Dr H. Chanzy for providing *Valonia* and tunicin samples and for his stimulating and helpful discussion. The authors also thank Saint-Louis Sucre for the supply of sugar beet pulps.

## References

Attala, R. H., & VanderHart, D. L. (1984). Native cellulose: a composite of two distinct crystalline forms. *Science*, *223*, 283–285.

Blumenkrantz, N., & Asboe, H. G. (1973). New method for quantitative determination of uronic acids. *Analytical Biochemistry*, *54*, 484–489.

Chanzy, H., Imada, K., & Vuong, R. (1978). Electron diffraction from the primary wall of cotton fibers. *Protoplasma*, *94*, 299–306.

Chanzy, H., Imada, K., Mollard, A., Vuong, R., & Barnoud, F. (1979). Crystallographic aspects of sub-elementary cellulose fibrils occurring in the wall of Rose cells cultured in vitro. *Protoplasma*, *100*, 303–316.

Dinand, E., Chanzy, H., Vignon, M.R., Vincent, I., Maureaux, A. (1995). Cellulose microfibrillée et son procédé d'obtention a partir des pulpes de betteraves sucrières. French Patent, 9501460.

Dinand, E., Chanzy, H., & Vignon, M. R. (1996). Parenchymal cell cellulose from sugar beet pulp: preparation and properties. *Cellulose*, *3*, 183–188.

Earl, W. L., & VanderHart, D. L. (1981). Observation by high-resolution carbon-13 Nuclear Magnetic Resonance of cellulose I related to morphology and crystal structure. *Macromolecules*, *14*, 570–574.

Ferrige, A. G., & Lindon, J. C. (1978). Resolution enhancement in FT-NMR through the use of a double exponential function. *Journal of Magnetic Resonance*, *31*, 337–340.

Frey-Wyssling, A. (1954). The fine structure of cellulose microfibrils. *Science*, *119*, 80–82.

Hill, D. J. T., Le, T. T., & Whittaker, A. K. (1994). A technique for the

quantitative measurements of signal intensities in cellulose-based transformer insulators by $^{13}$C CPMAS NMR. *Cellulose*, *1*, 237–247.

Horii, F., Yamamoto, H., Kitamaru, R., Tanahashi, M., & Higuchi, T. (1987). Transformation of native cellulose crystals induced by saturated steam at high temperatures. *Macromolecules*, *20*, 2946–2949.

Laivins, G. V., & Scallan, A. M. (1993). The mechanism of hornification of wood pulps. In C. F. Baker (Ed.), *Products of Papermaking*, (pp. 1235). Pira: Leatherhead.

Larsson, P. T., Westermark, U., & Iversen, T. (1995). Determination of the cellulose Iα allomorph content in a tunicate cellulose by CP/MAS $^{13}$C-NMR spectroscopy. *Carbohydrate Research*, *278*, 339–343.

Larsson, P. T., Wickholm, K., & Iversen, T. (1997). A CP/MAS $^{13}$C NMR investigation of molecular ordering in celluloses. *Carbohydrate Research*, *302*, 19–25.

Lenholm, H., Larsson, T., & Iversen, I. (1994). Determination of cellulose Iα and Iβ in lignocellulosic materials. *Carbohydrate Research*, *261*, 119–131.

Maciel, G. E., Kolododziejski, W. L., Bertran, M. S., & Dale, B. E. (1982). $^{13}$C NMR and order in cellulose. *Macromolecules*, *15*, 686–687.

Newman, R. H. (1997). Crystalline forms of cellulose in the silver tree fern *Cyathea dealbata*. *Cellulose*, *4*, 269–279.

Newman, R. H., & Hemmingson, J. A. (1990). Determination of the degree of cellulose crystallinity in wood by carbon-13 nuclear magnetic resonance spectroscopy. *Holzforschung*, *44*, 351–355.

Newman, R. H., & Hemmingson, J. A. (1994). Carbon-13 NMR distinction between categories of molecular order and disorder in cellulose. *Cellulose*, *2*, 95–110.

Newman, R. H., Ha, M-A., & Melton, L. D. (1994). Solid state $^{13}$C NMR investigation of molecular ordering in the cellulose of apple cell walls. *Journal of Agricultural Food Chemistry*, *42*, 1402–1406.

Newman, R. H., Davies, L. M., & Harris, P. J. (1996). Solid-state $^{13}$C Nuclear Magnetic Resonance characterization of cell walls of *Arabidopsis thaliana*leaves. *Plant Physiology*, *111*, 475–485.

O'Sullivan, A. (1997). Cellulose: the structure slowly unravels. *Cellulose*, *4*, 173–207.

Pfeffer, P. E. (1984). High resolution solid-state $^{13}$C NMR and its applications in carbohydrate chemistry. *Journal of Carbohydrate Chemistry*, *3*, 613–639.

Selvendran, R. R., March, J. F., & Ring, S. G. (1979). Determination of aldoses and uronic acids content of vegetable fibers. *Analytical Biochemistry*, *96*, 282–292.

Sugiyama, J., Persson, J., & Chanzy, H. (1991). Combined infrared and electron diffraction study of the polymorphism of native cellulose. *Macromolecules*, *24*, 2461–2466.

Teeäär, R., Serimaa, R., & Paakkari, T. (1987). Crystallinity of cellulose as determined by CP/MAS NMR and XRD methods. *Polymer Bulletin*, *17*, 231–237.

VanderHart, D. L., & Atalla, R. H. (1984). Studies of microstructure in native cellulose using solid-state $^{13}$C NMR. *Macromolecules*, *17*, 1465–1472.

Wormald, P., Wickholm, K., Larsson, P. T., & Iversen, T. (1996). Conversion between ordered and disordered cellulose, effects of mechanical treatment followed by cyclic wetting and drying. *Cellulose*, *3*, 141–152.

Yamamoto, H., & Horii, F. (1993). CP/MAS $^{13}$C NMR analysis of the crystal transformation induced for *Valonia*cellulose by annealing at high temperature. *Macromolecules*, *26*, 1313–1317.